Mon. Not. R. Astron. Soc. **000**, 1–10 (2008) Printed 24 July 2008 (MN LATEX style file v2.2)

Absolute Dimensions and Apsidal Motion of the Eccentric Binary V731 Cephei

V. Bakış[1⋆], M. Zejda[2], İ. Bulut[1], M. Wolf[3], S. Bilir[4], H. Bakış[1], O. Demircan[1], J. W. Lee[5], M. Šlechta[6], B. Kučerová[2]

[1] *Çanakkale Onsekiz Mart Univ. Observatory, Terzioğlu Campus, TR-17040, Çanakkale, Turkey*
[2] *Institute of Theoretical Physics and Astrophysics, Masaryk University, Kotlářská 2, CZ-611 37 Brno, Czech Republic*
[3] *Astronomical Institute, Faculty of Mathematics and Physics, Charles University Prague, V Holešovičkách 2, CZ-182 00 Praha 8, Czech Republic*
[4] *Istanbul University Science Faculty, Department of Astronomy and Space Sciences, 34119, University-Istanbul, Turkey*
[5] *Korea Astronomy and Space Science Institute, Daejeon 305-348, Korea*
[6] *Astronomical Institute, Academy of Sciences, CZ-251 65 Ondřejov, Czech Republic*

24 July 2008

ABSTRACT

A detailed analysis of new and existing photometric, spectroscopic and spatial distribution data of the eccentric binary V731 Cep was performed. Spectroscopic orbital elements of the system were obtained by means of cross-correlation technique. According to the solution of radial velocities with $UBVR_c$ and I_c light curves, V731 Cep consists of two main-sequence stars with masses M_1=2.577 (0.098) $M_\odot$, M_2=2.017 (0.084) $M_\odot$, radii R_1=1.823 (0.030) $R_\odot$, R_2=1.717 (0.025) $R_\odot$, and temperatures T_{eff1}=10700 (200) K, T_{eff2}=9265 (220) K separated from each other by a=23.27 (0.29) $R_\odot$ in an orbit with inclination of 88°.70 (0.03). Analysis of the O–C residuals yielded a rather long apsidal motion period of U=10000(2500) yr compared to the observational history of the system. The relativistic contribution to the observed rates of apsidal motion for V731 Cep is significant (76 per cent). The combination of the absolute dimensions and the apsidal motion properties of the system yielded consistent observed internal structure parameter ($\log\bar{k}_{2,obs} = -2.36$) compared to the theory ($\log\bar{k}_{2,theo} = -2.32$). Evolutionary investigation of the binary by two methods (Bayesian and evolutionary tracks) shows that the system is t =133(26) Myr old and has a metallicity of $[M/H] = -0.04(0.02)$ dex. The similarities in the spatial distribution and evolutionary properties of V731 Cep with the nearby ($\rho \sim 3°.9$) open cluster NGC 7762 suggests that V731 Cep could have been evaporated from NGC 7762.

Key words: binaries: eclipsing – binaries: early-type – stars: evolution – stars: fundamental parameters – stars: individual (V731 Cephei)

1 INTRODUCTION

Study of eclipsing binaries is still the most effective way of determining the absolute parameters of stars, especially from the spectroscopic and photometric analysis of detached double-lined eclipsing binaries, masses and radii of the components can be obtained with a precision of ∼1 per cent (e.g. Southworth et al. 2005; Bakış et al. 2008), the limit precision for stellar evolutionary tests (Andersen 1991). Among the stars, those in the upper main sequence band are particularly useful in empirical tests of the convection formulae used in various evolution codes, while systems containing unevolved stars are useful in testing opacity and metallicity effects in near-ZAMS (Zero Age Main Sequence) models. V731 Cep, the binary discussed in the present paper, is of the latter type.

The variability of V731 Cep (GSC 4288 0168; brightness at maximum V∼10.5 mag; orbital period P∼6.06 d) was discovered by Bakış et al. (2003) (hereafter B03). A brief history of V731 Cep was given by Bakış et al. (2007) (hereafter B07) who presented photometric light curves in BVR_c and I_c bands and limited spectroscopic observations. Within the scope of a project to study close eclipsing bina-

⋆ bakisv@comu.edu.tr

ries of SB2 type, we were able to obtain new times of minima as well as new spectroscopic data for V731 Cep.

The system has an eccentric orbit ($e = 0.0165$), which makes it an important astrophysical tool for the investigation of internal structures of its components, if the rotation period of the apsides is precisely determined. The apsidal motion period together with system geometry allow the computation of the observed internal structure constant (ISC) to be compared with theoretical internal structure computations. The primary motivation for the present paper is to obtain the parameters of the close binary system V731 Cep, to discuss the evolutionary status of the system using the system parameters with the latest evolutionary models, and to investigate the apsidal motion of the orbit for estimation of the internal structures of the component stars.

2 OBSERVATIONS

2.1 Photometry

As the photometric data presented by B07 are precise enough (rms scatter of ∼0.008 mag) for light curve analysis with nearly complete phase coverage of the data, apart from new times of minima observations, no new photometric observations were performed in this study. The details of the photometric observations and their reduction are given in detail by B07. The standard $UBVR_c$ and I_c magnitudes of the comparison and check stars in the same CCD field with V731 Cep were derived using transformation coefficients obtained by B07, and are given in Table 1 together with near-infrared magnitudes from the Two Micron Sky Survey (*2MASS*, Cutri et al. 2003). *2MASS* magnitudes in Table 1 correspond to phases where the light was at maximum.

The phasing of the photometric data in the present paper was made using the updated ephemeris for primary minimum given in Eq. 1. This ephemeris together with the ephemeris for the secondary minimum are given in B07. In Fig. 1, the primary and secondary minima of the light curve is plotted together with $(B - V)$ colours.

$$MinI(HJD) = 2453137.4425(2) + 6.068456(2) \times E \qquad (1)$$

The difference between the periods given in Eq. 1 and in the ephemeris for the secondary minimum (B07) is clearly outside the observational error box, which of course indicates an apsidal motion in the system. To study apsidal motion, new times of minima for V731 Cep were obtained and are given in Table 2 together with the telescope and observatory information. During the (additional) eclipse timing observations at Ondřejov Observatory, one of the two available CCD cameras (SBIG ST-8 or Apogee AP-7) were used, while SBIG ST-10XME and ST-7 CCD cameras were employed at ÇOMÜ and Brno Observatories, respectively. The reduction of all photometric data was performed using C-Munipack[1] free software under GNU General Public License. The times of minima have been calculated according to the Kwee–van Woerden method (Kwee & van Woerden 1956). In addition to new times of minima observations, all available historical eclipse timings are also listed in Table 2.

[1] http://integral.physics.muni.cz/cmunipack/

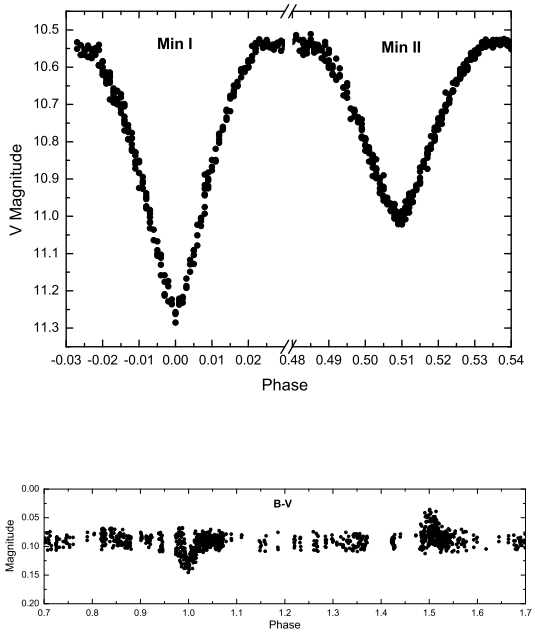

Figure 1. Primary and secondary minimum in V-band *(upper panel)*. $B - V$ colour vs orbital phase *(lower panel)*.

2.2 Spectroscopy

Spectroscopic observations of V731 Cep were made using a Coudé spectrograph with 2.0-m reflector at Ondřejov Observatory, equipped with a SITe-005 800×2000 CCD. The spectra cover the region from 6280 Å to 6720 Å, with a linear dispersion of 17 Å/mm and two-pixel resolution of 12700. Each frame was processed using IRAF[2] software according to normal procedures of bias and dark substraction, flat-field division, rectification of background continuum and wavelength calibration.

A total of seven spectra were obtained between 2005-2006. The exposure times of a single observation were arranged not to exceed 8000s which corresponds to 0.015 in phase and to have an average signal-to-noise (S/N) ratio of ∼100 in continuum near H_α line. Two spectra taken have S/N ratio below 100 due to bad weather conditions. The information on each individual spectrum is given in the journal of spectroscopic observations presented in Table 3.

3 APSIDAL MOTION

The very slow apsidal motion of V731 Cep was detected and studied by means of the O–C diagram analysis. All available times of minimum were collected from the literature and are listed in Table 2 together with the new times of minima. We used the methods of Giménez & García-Pelayo (1983)

[2] IRAF is distributed by the National Optical Astronomy Observatories, which is operated by the Association of Universities for Research in Astronomy, Inc. (AURA) under cooperative agreement with the National Science Foundation.

Table 1. Standard magnitudes for V731 Cep and the comparison stars. Infrared *J, H* and K_s magnitudes are taken from *2MASS* point sources catalogue (Cutri et al. 2003).

GSC No	Phase	U	B	V	R_c	I_c	J	H	K_s
V731 Cep	0.00	–	11.38	11.25	11.14	11.11	-	-	-
(4288 0186)	0.25	10.59	10.63	10.54	10.46	10.42	10.095	10.049	10.021
	0.51	–	11.07	11.02	10.94	10.91	-	-	-
4288 0052	–	10.95	10.95	10.86	10.76	10.70	10.329	10.297	10.252
4288 0062	–	11.57	11.42	11.14	10.88	10.70	-	-	-
4288 0220	–	13.02	12.34	11.33	10.72	10.24	9.112	8.593	8.475
4288 0241	–	12.65	11.97	11.53	11.23	11.02	10.428	10.198	10.123

Table 2. New and historical times of minima of V731 Cep.

HJD (-2400000)	Uncertainty	Weight	Filter	Type	Reference / Telescope and Observatory
52515.4840	0.0045	3	clear	sec	B03
52560.9401	0.0006	10	BVR_cI_c	pri	Lee et al. (2007)
52591.2817	0.0001	10	clear	pri	B03
52594.3767	0.0014	3	clear	sec	B03
52791.5388	0.0003	3	clear	pri	Bakış et al. (2005a)
52861.3828	0.0003	10	clear	sec	Bakış et al. (2005a)
52864.3624	0.0006	10	clear	pri	Bakış et al. (2005a)
52864.3626	0.0019	5	I	pri	Zejda (2004)
52864.3621	0.0028	5	V	pri	Zejda (2004)
52864.3630	0.0028	5	R	pri	Zejda (2004)
52867.4522	0.0014	5	clear	sec	Bakış et al. (2005a)
52867.4505	0.0013	10	RI	sec	Pejcha (2005)
52879.5890	0.0012	10	clear	sec	Bakış et al. (2005a)
52934.2099	0.0005	3	clear	sec	Bakış et al. (2005a)
52949.3211	0.0002	10	R_c	pri	0.65 m reflector, primary focus, Ondřejov Obs.
52967.5258	0.0004	10	clear	pri	Bakış et al. (2005a)
53134.4590	0.0004	3	BVR_cI_c	sec	Bakış et al. (2005a)
53137.4431	0.0005	10	BVI_c	pri	Bakış et al. (2005a)
53213.3532	0.0003	10	BV	sec	Bakış et al. (2005a)
53219.4218	0.0004	10	BVR_cI_c	sec	Bakış et al. (2005a)
53577.4608	0.0003	10	BVR_cI_c	sec	Bakış et al. (2005b)
53580.4393	0.0004	10	R_c	pri	0.65 m reflector, primary focus, Ondřejov Obs.
53580.4396	0.0002	10	BVR_cI_c	pri	Bakış et al. (2005b)
53753.4455	0.0003	10	BVR_cI_c	sec	B07
53756.4251	0.0003	10	BVR_cI_c	pri	B07
53929.4303	0.0004	10	R_c	sec	0.65 m reflector, primary focus, Ondřejov Obs.
53941.5675	0.0002	10	VR_c	sec	0.40 m, Newton, Brno Obs.
53944.54653	0.00012	20	R_c	pri	0.65 m reflector, primary focus, Ondřejov Obs.
54378.4960	0.0010	3	clear	sec	0.30 m, Cassegrain-Schmidt, ÇOMÜ Obs.
54387.54272	0.00008	10	VR_c	pri	0.40 m, Newton, Brno Obs.
54536.2750	0.0006	10	VR_cI_c	sec	0.30 m, Cassegrain-Schmidt, ÇOMÜ Obs.

Table 3. Journal of spectroscopic observations. Date column refers to the local date of the start of night. Signal-to-noise S/N ratio refers to the continuum near H_α.

No	Frame	HJD (-2400000)	Date	Phase (ϕ)	S/N	Exp. Time (s)
1	oj090013.fit	53653.32491	09.10.2005	0.010	50	7500
2	pi090066.fit	53988.61624	10.09.2006	0.262	65	7000
3	oh290012.fit	53612.44057	29.08.2005	0.273	115	7500
4	pi100032.fit	53989.50350	11.09.2006	0.408	100	7200
5	oh300036.fit	53613.47736	30.08.2005	0.444	100	8000
6	oi240017.fit	53638.33066	24.09.2005	0.540	125	7200
7	oi070028.fit	53621.42400	07.09.2005	0.754	115	7200

Table 4. Apsidal motion elements of V731 Cep. Errors in brackets denote the last digits.

Parameter	Unit	Value
T_0	HJD	2453137.44241(5)
$P_{\rm s}$	d	6.0684499(35)
$P_{\rm a}$	d	6.0684600(25)
e		0.0165
$\dot{\omega}$	$^\circ$/cycle	0.00060(15)
ω_0	$^\circ$	29.87(42)
U	yr	10000(2500)

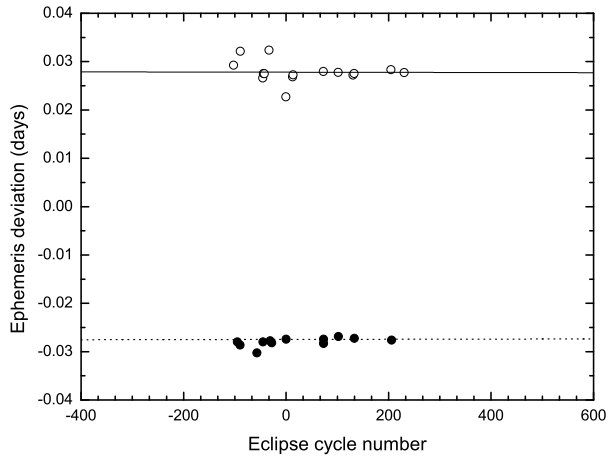

Figure 2. Ephemeris curve for V731 Cep obtained with the parameters in Table 4. Filled and open symbols represent the residuals from the primary and secondary minimum, respectively.

and Lacy (1992) independently with similar results given in Table 4. All precise CCD times of minima were used with a weight of 20 or 10, less accurate measurements were assigned with weights of 5 or 3.

Since the eccentricity is only weakly constrained by the observations in this case, we adopted a value of $e = 0.0165$ from the light-curve solutions given in Table 7. For the inclination angle we used $i = 88^\circ.7$, from the light curve solutions. The results are given in Table 4. In this table, ($P_{\rm a}$) and ($P_{\rm s}$) are the anomalous and sidereal periods, respectively. The zero epoch is given (T_0) and the corresponding position of the periastron is represented by (ω_0). The apsidal motion rate ($\dot{\omega}$) that we obtained seems to be statistically significant, $\dot{\omega} = 0.00060$ (0.00015) $^\circ$ cycle^{-1}. This corresponds to an apsidal period of $U = 10000(2500)$ yr. The ephemeris curve is shown in Fig. 2, along with the residuals from the observed primary and secondary minima.

We tested the stability of the results with respect to our arbitrarily chosen weighting scheme. It turned out that the resulting parameters show some dependence on the weighting. For this reason, as well as for other reasons discussed below, the results must be considered preliminary and less certain.

Table 5. RVs of the components measured by TODCOR.

Time HJD	Phase ϕ	RV_1 (km s^{-1})	RV_2 (km s^{-1})
2453653.32491	0.010	—	-5.7(1.2)
2453988.61624	0.262	-83.8(2.0)	107.3(3.2)
2453612.44057	0.273	-81.4(1.2)	109.3(1.8)
2453989.50350	0.408	-47.0(1.4)	57.1(2.1)
2453613.47736	0.444	-27.7(1.2)	43.8(1.4)
2453638.33066	0.540	14.2(1.3)	-28.0(1.7)
2453621.42400	0.754	88.2(1.2)	-106.1(1.5)

4 RADIAL VELOCITIES AND SPECTROSCOPIC ORBIT

The method we adopted for radial velocity (RV) measurements was the two-dimensional cross-correlation (TODCOR) of the observed spectra with two synthetically produced template spectra. The algorithm of TODCOR was developed by Zucker & Mazeh (1994) and has been efficiently applied to multiple-component spectra of late-type double-lined spectroscopic binaries (Latham et al. 1996; Metcalfe et al. 1996, among others) and more recently to short-period early-type binaries (Gonzales & Lapasset 2003; Southworth & Clausen 2007). Basically, TODCOR calculates two-dimensional cross-correlation function (CCF) from one observed and two template spectra in re-binned log λ space and then locates the maximum of the CCF. We re-binned our observed and template spectra so that each pixel corresponded to 2.2 kms^{-1}. The template spectrum of each component was synthetically produced using the appropriate model atmosphere grids of Kurucz (1993) for each component's temperature, surface gravity and projected rotational velocity values, as listed in Table 8. The two template spectra are shown in Fig. 3 together with the Si II doublets (6347.091 Å, 6371.359 Å) which were used for RV measurement by TODCOR. The RVs of the components were computed from the 2-dimensional CCFs with the highest score which is formed by combining the one dimensional CCFs of the shifted and rescaled template spectra with the observed one. The RVs measured and their errors are presented in Table 5.

Using the TODCOR RVs, the orbital solution was performed by least-squares orbital fitting. The orbital period of P=6.068456 days (Eq. 1) was fixed while the velocity semi-amplitudes $K_{1,2}$, systemic velocity V_γ and the conjunction time (starting from 2453137.4425 HJD) were converged in the least-squares solution. Due to the small number of observations, the eccentricity (e) and the longitude of periastron (ω) parameters were also fixed at the values obtained from the light curve analysis results listed in Table 7. The radial velocity at phase ϕ=0.01 was not used due to inaccurate RV reading from the blended spectra of the components. In order to avoid systematic effects in the orbital fitting due to the proximity of the components, although they are small, the effect of proximity was also considered using the system geometry obtained in §5.2. The orbital parameters adopted from the least-square fitting are listed in Table 6 and the orbital fitting to RVs is shown in Fig. 4.

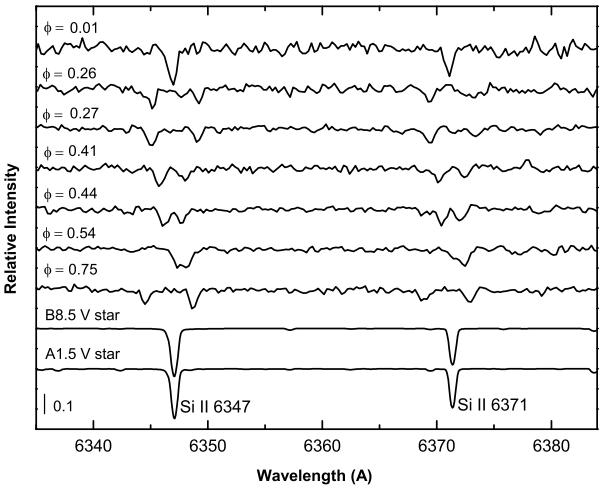

Figure 3. Si II doublets (6347.091 Å, 6371.359 Å) at different orbital phases indicated. Synthetic spectra of the components are shown below the observations and indicated with "B8.5 V star" for primary and "A1.5 V star" for secondary components. For clarity, the intensity has been shifted and wavelength re-scaled.

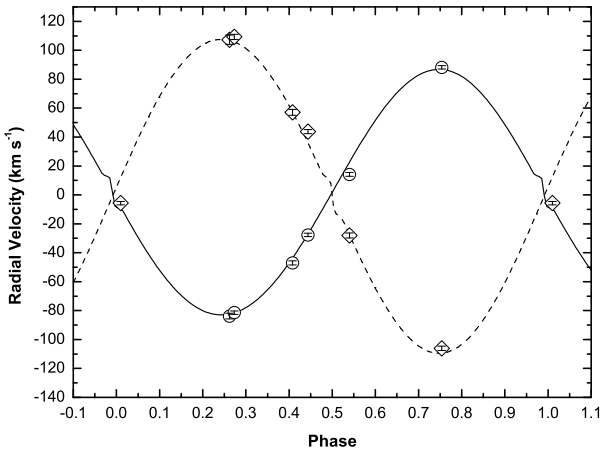

Figure 4. RVs and the spectroscopic orbital solution. Primary and secondary RVs are shown with circles and diamonds, respectively. Error of each individual RV measurement is indicated with bars in RV symbols. Theoretical RV curves including proximity and eclipse effects are shown for the primary (solid line) and secondary components (dashed line).

Table 6. Spectroscopic orbital solution adopted from the analysis of TODCOR RVs. Parameters without errors were fixed during the solutions.

Parameter	Value
P (d)	6.068456
T_0 (HJD-2453137)	0.322(0.030)
K_1 (km s^{-1})	85.18(1.72)
K_2 (km s^{-1})	108.84(1.73)
q (K_1/K_2)	0.783(0.024)
V_γ (km s^{-1})	0.62(0.94)
e	0.0165
w ($^\circ$)	25
$m_1 \sin^3 i$ ($M_\odot$)	2.575(0.098)
$m_2 \sin^3 i$ ($M_\odot$)	2.015(0.084)
$a \sin i$ ($R_\odot$)	23.26(0.29)

5 MODELLING OF LIGHT CURVES

5.1 Reddening toward the system

The first element needed in the light curve modelling is an estimate of the effective temperature of the primary component. The Q-method of Johnson & Morgan (1953) was used with the UBV indices given in Table 1. Due to unavailability of U-magnitudes for eclipses, the colours of the combined light (ϕ=0.25) were used to determine a Q value of $-0.10(0.03)$. According to the relation $(B-V)_0$=-0.009+$0.337Q$ (Johnson & Morgan 1953), one can determine the unreddened colour index of $(B-V)_0$=$-0.04(0.02)$. From the difference between the colours at 0.25 and 0.51 phases, the colour of the primary component is derived to be $(B-V)_0$=$-0.07(0.02)$ which corresponds to a spectral type of B8.5V with $E(B-V)$=0.13(0.03) colour excess.

The reddening obtained from the Q-method was checked by using Red Clump (RC) stars in this area. Red clump giants have long been proposed as standard candles. They have a very narrow luminosity function and constitute a compact and well-defined clump in an HR diagram, particularly in the infrared. Furthermore, as they are relatively luminous, they can be identified even at large distances from the Sun. The absolute magnitude (M_K) and intrinsic colour, $(J-K_s)_0$, of the red clump giants are well established (Alves 2000; Grocholski & Sarajedini 2002; Salaris & Girardi 2002; Pietrzynski et al. 2003). Here, we assume an absolute magnitude for the red clump population of -1.62(0.03) mag and an intrinsic colour of $(J-K_S)_0 = 0.7$ mag.

In order to make the reddening estimation in the direction of V731 Cep, the J, H and K_s magnitudes of the sources in the 1 square degree field, whose central galactic coordinates are ($l = 115^\circ, b = 2^\circ$), were obtained from *2MASS* point sources catalogue (Cutri et al. 2003). The isolation of the red clump sources in the star field was made by using theoretical traces to define the limits of the K-giant branch on the colour magnitude diagrams (CMDs), without any further implication in the method -the traces were obtained for different stellar types by using a double exponential approximation to the interstellar extinction according to the updated "SKY" model (Wainscoat et al. 1992).

The maxima of the RC distribution, obtained via Gaussian fitting at different magnitude bins are shown in Fig. 5 (see Lopez-Corredoira et al. 2002, or Cabrera-Lavers et al. 2005 for further details of the method), and the distance of RC stars in the direction of V731 Cep and their absorption on K-band are shown in Fig. 6. It is seen that the distance between RC stars in the direction of the star field and the Sun is $1 < d \leqslant 7$ kpc. The average absorption in the K band calculated from the RC stars closest ($1 < d < 1.5$ kpc) to V731 Cep system is $A(K_s) = 0.279$.

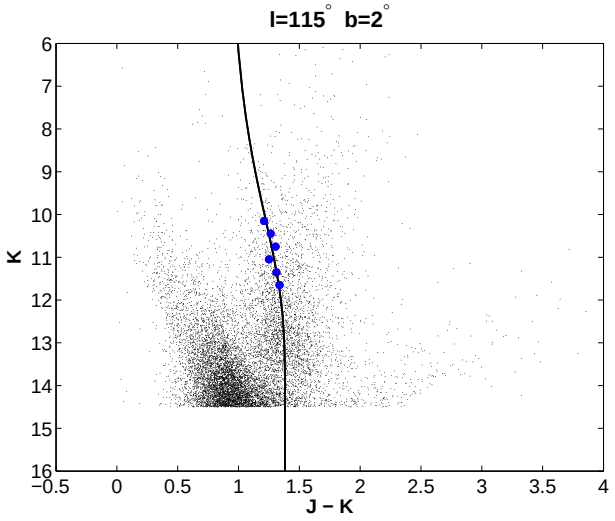

Figure 5. Maxima of the RC stars for different magnitude bins and the theoretical trace for a RC star (spectral type K2-3III) obtained from the SKY model by assuming a double exponential distribution for the dust in the Galaxy.

By using $A(K_s) = 0.382 \times E(B-V)$ relation, the colour excess in the direction was calculated as $E(B-V) = 0.730$ and total absorption in V band was calculated as $A(V) = 2.263$. To reduce this colour excess to the V731 Cep system, we applied the following equation (Bahcall & Soneria 1980):

$$A_d(b) = A_{RC}(b)\left[1 - exp\left(\frac{-\mid d\ sin(b)\mid}{H}\right)\right]. \quad (2)$$

Here, b and d are the Galactic latitude and distance of V731 Cep, respectively. H is the scaleheight for the interstellar dust adopted as 134 pc (Drimmel et al. 2003), d = 809 pc, and $A_{RC}(b)$ and $A_d(b)$ are the total absorptions obtained from the SKY model for RC stars and for the distance to the V731 Cep, respectively. According to Eq. 2, the total absorption in V-band and colour excess for the distance to the V731 Cep are $A_d(b) = 0.477(0.090)$ and $E(B-V) = 0.154(0.029)$, respectively. The colour excess $E(B-V) = 0.154(0.029)$ which is found from RC stars is in good agreement with the $E(B-V) = 0.13(0.03)$ obtained from the Q-method. Hence, it seems fair to adopt confidently the unreddened colour of $(B-V)_0$=−0.07 mag as the intrinsic colour of the primary component. The intrinsic colour of the primary component corresponds to a spectral type of B8.5V (Fitzgerald 1970) with a temperature of 10700 K according to the calibration tables of Straižys & Kuriliene (1981).

5.2 Determination of the photometric elements

We performed a simultaneous analysis of the BVR_c and I_c light curves using the 2003 version of the Wilson-Devinney (Wilson & Devinney 1971; Wilson 1994; hereafter WD) program.

During the simultaneous fit with WD code, the adjustable parameters were the orbital semi-major axis (a), the orbital eccentricity (e), the longitude of periastron (ω), the orbital inclination (i), the temperature of the secondary component (T_{eff2}), surface potential of both components ($\Omega_{1,2}$), and the luminosity of the primary component in each band (L_1). The mass ratio (q) was taken from the spectroscopic orbital solution (§3) and was used as a fixed parameter during the analysis. An eccentric orbit was adopted, and the gravity brightening coefficients and bolometric albedos were set to unity in accordance with the radiative atmospheres of the components. The limb-darkening (LD) coefficients from the logarithmic LD-law were computed at each iteration from van Hamme (1993).

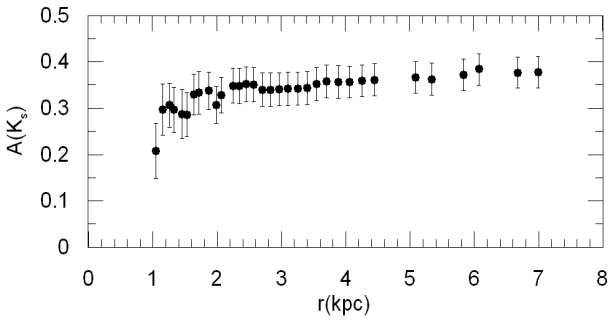

Figure 6. Extinction along the line of sight (A_K vs. r) for the field ($l = 115°, b = 2°$) obtained from the RC maxima in the CMD.

All observations in each band were weighted equally. Convergence of the fits was reached rapidly and tests from different starting points indicated the uniqueness of the solution. The final residual sum of squares (rss) are similar in all bands of the light curves, 0.038 in B, 0.040 in V, 0.033 in R_c and 0.042 in I_c. The resulting best fitting light curve elements are given in Table 7. The light curves with the best fitting model curves superimposed and the O–C residuals from the fits are shown in Fig. 7.

6 DISCUSSION

6.1 Absolute Dimensions and Distance of the System

Combination of spectroscopic orbital elements (Table 6) with light curve elements (Table 7) yields the absolute dimensions of the system, which are presented in Table 8. The adopted temperature T_{eff1}=10700 K and mass M_1=2.577$M_\odot$ of the primary component correspond to the spectral type of a normal B8.5-type main sequence star, while the adopted temperature T_{eff2}=9265 K and mass M_2=2.017$M_\odot$ of the secondary component are in good agreement with the spectral type of a normal A1.5-type main sequence star (i.e. Straižys & Kuriliene 1981). However, the radii of the components, R_1=1.823$R_\odot$ and R_2=1.717$R_\odot$, are in better agreement with the same spectral type stars but at closer locations to ZAMS, suggesting a young age of the system, as determined in §6.2.

The synchronization time-scale for the component stars of the V731 Cep system is, following Zahn (1977), in the order of 15 Myr, which is smaller than the age of 120 Myr estimated from the isochrones (see §6.2). To compare the observed rotational velocities with the synchronization velocities listed in Table 8, we have modelled Si II doublets

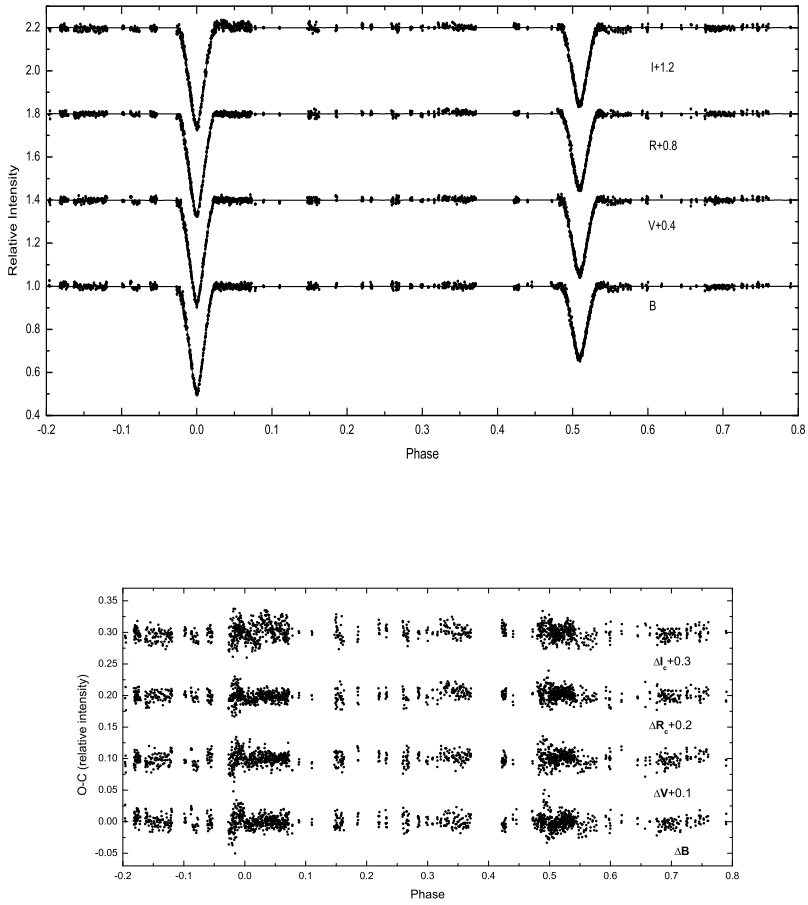

Figure 7. Theoretical model fits to the light curves of V731 Cep *(upper panel)*. O–C residuals from the theoretical fits *(lower panel)*.

(6347.091 Å, 6371.359 Å) with model atmosphere grids using ATLAS9 and SYNTHE codes under Linux (Kurucz 1993). The modeling yielded equatorial rotational velocities of V_{rot1}=19(3) km s^{-1} and V_{rot2}=18(3) km s^{-1} for the primary and secondary components, respectively. Although errors in the observed rotational velocities are in the order of 15 per cent, the synchronization velocities seem to be slightly below the observational measurements. The asynchronization of the components with the orbit should be confirmed by analyzing new spectra with a higher S/N ratio and more absorption lines in a larger spectral range.

Using the brightness of the system listed in Table 1 together with the light contributions of the components listed in Table 7, the intrinsic magnitudes of the components were calculated and are presented in Table 9. During the derivation of the intrinsic magnitudes, the interstellar extinction in B and V bands were adopted from the Q-method while the following relations of Fiorucci & Munari (2003) were used for the determination of extinction in R_c and I_c.

$$\begin{aligned}(R_c)_0 &= R_c - 2.494 \times E(B-V),\\ (I_c)_0 &= I_c - 1.753 \times E(B-V).\end{aligned} \quad (3)$$

where $(R_c)_0$ and $(I_c)_0$ are the de-reddened magnitudes.

The de-reddened visual apparent magnitude and optical absolute magnitude presented in Table 8 allowed us to derive a distance of 809(30) pc to the system. To compare the distance of V731 Cep system using a different method, a luminosity-colour relation (Bilir et al. 2008) which has been formed for detached binary systems with main-sequence components was used in this study. The near-infrared magnitudes of the system were taken from the *2MASS* Point Sources Catalogue of Cutri et al. (2003) and are shown in Table 1. For de-reddenig near-infrared magnitude and colours of the system, the following formulae (Bilir, Güver, Aslan 2006; Ak et al. 2007; Bilir et al. 2008) were used:

$$\begin{aligned}J_o &= J - 0.884 \times E(B-V),\\ (J-H)_o &= (J-H) - 0.322 \times E(B-V),\\ (H-K_s)_o &= (H-K_s) - 0.187 \times E(B-V).\end{aligned} \quad (4)$$

All the colours and magnitude with subscript "0" show the de-reddened ones. The colour excess $E(B-V) = 0.13$ was estimated in a direction to V731 Cep by using Q-method (see §5.1). The near-infrared absolute magnitude

Table 8. Close binary stellar parameters of V731 Cep. Errors of parameters are given in parenthesis.

Parameter	Symbol	Primary	Secondary
Mass ($M_\odot$)	M	2.577(0.098)	2.017(0.084)
Radius ($R_\odot$)	R	1.823(0.030)	1.717(0.025)
Separation ($R_\odot$)	a	23.27(0.29)	
Surface gravity (cgs)	$\log g$	4.304(0.011)	4.273(0.011)
Integrated visual magnitude (mag)	V	10.54(0.01)	
Integrated colour index (mag)	$B-V$	0.09(0.01)	
Colour excess (mag)	$E(B-V)$	0.13(0.03)	
Visual absorption (mag)	A_V	0.40	
Intrinsic colour index (mag)	$(B-V)_0$	-0.04(0.02)	
Component intrinsic colour index (mag)	$(B-V)$	-0.073(0.020)	0.016(0.020)
Temperature (K)	T_{eff}	10700(200)	9265(220)
Spectral type	Sp	B8.5 V	A1.5 V
Luminosity ($L_\odot$)	$\log L$	1.618(0.035)	1.292(0.043)
Computed synchronization velocities (km s^{-1})	V_{synch}	15.6(0.2)	14.3(0.2)
Observed rotational velocities (km s^{-1})	V_{rot}	19(3)	18(3)
Bolometric magnitude (mag)	M_{bol}	0.705(0.088)	1.519(0.108)
Velocity amplitudes (km s^{-1})	$K_{1,2}$	85.18(1.72)	108.84(1.73)
Absolute visual magnitude (mag)	M_v	1.104(0.054)	1.631(0.070)
Bolometric correction (mag)	BC	-0.399	-0.112
Distance (pc)	d	809(30)	
Systemic velocity (km s^{-1})	V_γ	0.62(0.94)	
Parallax (mas)	π	1.236(0.044)*	
Proper motion (mas yr^{-1})	$\mu_\alpha cos\delta$, μ_δ	-1.5 (2.6), -3.1 (2.5)**	
Space velocities (km s^{-1})	U, V, W	7.59(9.03), 4.71(4.31), -9.75(9.62)	

** In this study.*
*** NOMAD Catalog (Zacharias 2005).*

Table 7. Results from the simultaneous solution of BVR_c and I_c-band light curves of V731 Cep system. Adjusted and fixed parameters are presented in separate panels of the table.

Parameter	Value
Adjusted parameters:	
$T_{eff2}(K)$	9265(20)
$L_1/L_{1+2}(B)$	0.639(0.008)
$L_1/L_{1+2}(V)$	0.620(0.008)
$L_1/L_{1+2}(R_c)$	0.613(0.008)
$L_1/L_{1+2}(I_c)$	0.604(0.008)
Ω_1	13.24(0.12)
Ω_2	11.75(0.08)
r_1(mean)	0.0805(0.0008)
r_2(mean)	0.0738(0.0005)
$i(^o)$	88.70(0.03)
e	0.0165(0.0005)
$w(^o)$	25(2)
Fixed parameters:	
A_1=A_2	1.0
g_1=g_2	1.0
$T_{eff1}(K)$	10700
q	0.783
$x_1(B,V,R_c,I_c)$	0.678, 0.581, 0.496, 0.396
$y_1(B,V,R_c,I_c)$	0.338, 0.290, 0.246, 0.195
$x_2(B,V,R_c,I_c)$	0.733, 0.630, 0.534, 0.425
$y_2(B,V,R_c,I_c)$	0.325, 0.286, 0.249, 0.201
F_1=F_2	1.034
χ^2_{min}	0.149

Table 9. De-reddened magnitudes of stars in V731 Cep system.

	B	V	R_c	I_c	Err.
Primary	10.59	10.66	10.67	10.74	0.02
Secondary	11.21	11.19	11.17	11.20	0.02

of V731 Cep system was estimated by the luminosity-colour relation, $M_J = 5.228(J-H)_o + 6.185(H-K_s)_0 + 0.608$, of Bilir et al. (2008) and the distance of the system calculated as 733(50) pc by using the photometric parallaxes method. The photometric distance of 809(30) pc given in Table 8 is consistent with the 733(50) pc distance estimated by luminosity-colour relation obtained for detached binary systems.

6.2 Internal Structure

Binary systems with apsidal motion allow us to determine the ISC, which is an important parameter of stellar evolution models. The observed apsidal motion period of U = 10000(2500) yr, corresponding to a total rate of $\dot{\omega}$ = 0.00060(0.00015) $^\circ$ cycle^{-1} was obtained in §6. The relativistic contribution to the apsidal motion in case of V731 Cep is substantial $\dot{\omega}_{rel} = 0.00045$ $^\circ$ cycle^{-1}, or about 75 per cent of the total observed rate (Giménez 1985). After correcting for this effect, an average ISC was derived to be $\log \bar{k}_{2,obs} = -2.36$ under the assumption that the component stars rotate pseudosynchronously. This value is in very good agreement with the theoretical prediction of $\log \bar{k}_{2,theo} = -2.34$ according to new evolutionary models of Claret (2004) with

the standard chemical composition of (X,Z) = (0.70, 0.02). It should, however, be noted that the present apsidal motion solution is still tentative due to relatively short observational history of V731 Cep compared to the apsidal motion period. Therefore, accurate eclipse timings are strongly needed in a decade or more in order to say more definite on the apsidal motion parameters and the related ISC.

6.3 Evolutionary Stage and Age of the System

We investigated the evolutionary status of the system by means of the Bayesian method and constructing an H-R diagram for the component masses in log T_{eff}-log L plane. We used a slightly modified version of the Bayesian estimation method idealized by Jørgensen & Lindegren (2005), which is designed to avoid statistical biases and to take error estimates of all observed quantities into consideration. Estimation of age and metal abundance of the components was made by using the web interface[3] based on the Bayesian method of da Silva et al. (2006). Including their errors, the effective temperatures, visual brightness, metal abundance of components and distance to the system were the parameters used in the web interface to obtain the best matching model parameters (i.e. surface gravity (log g), radii ($R_{1,2}$), masses ($M_{1,2}$) and age of components ($t_{1,2}$)) to Padova isochrones by the Bayesian method. Since the metal abundance of the components was initially not known, a range of metal abundance (i.e. $-0.10 < [M/H] < +0.10$ dex) was selected and the values in this range were used with 0.02 dex steps. The output model parameters for each component were compared by means of χ^2 test with the absolute dimensions of the components listed in Table 8. Consequently, the minimum χ^2 yielded simultaneously the metal abundance and age of the components as $[M/H]_1 = -0.06(0.02)$ dex and $t_1 = 116(15)$ Myr for the primary and $[M/H]_2 = -0.02(0.02)$ dex and $t_2 = 150(15)$ Myr for the secondary component. From these values, we adopted the mean metal abundance and mean age of the system to be $[M/H] = -0.04(0.02)$ dex and $t = 133(26)$ Myr, respectively.

Interpretation of the evolutionary status of V731 Cep requires also the construction of H-R diagrams using the latest theoretical evolutionary models. In Fig. 8, the components of V731 Cep are shown in the log T_{eff}-log L plane together with Yonsei-Yale (Y2) evolutionary tracks (Yi, Demarque, Kim et al. 2001; hereafter YDK) for different masses. Evolutionary tracks for the exact masses of the components were also computed using the code provided by YDK. Among the tracks computed for the exact masses with their errors, those with $[M/H]$=-0.024 dex (Z=0.0172) metallicity models match the locations of the components within the error limits in the log T_{eff}-log L plane. We also computed a set of isochrones using a metallicity of $[M/H]$= -0.024 dex in Y2 models. In Fig. 8, two isochrones (t =100 Myr and t =120 Myr) are plotted for comparison. It was found that 120 Myr age is the best fitting isochrone to the locations of both components. Although, the most reliable method of metal abundance determination is the atmosphere modeling of spectral lines, in the present study,

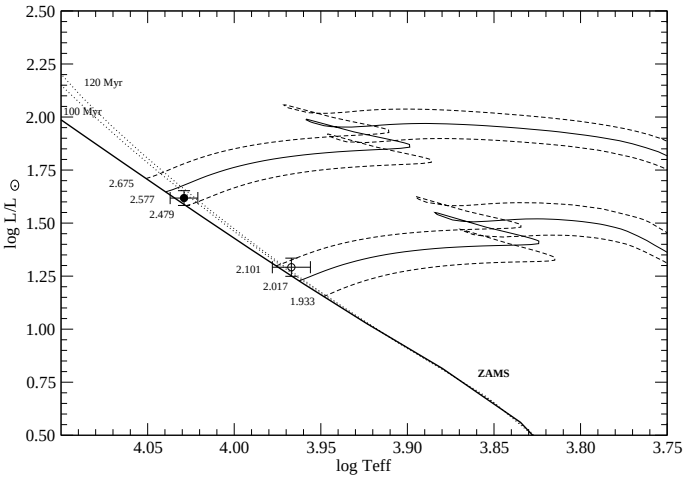

Figure 8. Evolutionary tracks for individual component masses and isochrone curves best matching the location of the components in log T_{eff} - log L plane. The primary and secondary stars are shown with filled and empty circles, respectively.

it seems fair to conclude that the two methods (Bayesian methods and evolutionary tracks) used for estimation of the metallicity and age of the system are in excellent agreement within the error limits. The metallicity we found for the components should be confirmed with the atmosphere modeling of metallic absorption lines in spectra taken in wider wavelength range.

6.4 Possible Origin of V731 Cep

One of the formation regions of early-type stars is open clusters. To find a possible formation region for V731 Cep, nearby young open clusters were investigated. Among others, NGC 7762 was found to be the closest open cluster and the most similar in chemical composition to V731 Cep. Chincarini (1966) estimated the distance of NGC 7762 to be 750 pc and the age 266 Myr. In a more recent study relating on the cluster, Patat & Carraro (1995) proposed a similar distance of 800 pc to NGC 7762. Nevertheless, Patat & Carraro (1995) estimated an older age for the cluster at 1.8 Gyr and less metallicity compared to the Sun. The age (133 Myr) we adopted for V731 Cep system seems to agree more with the age (266 Myr) that Chincarini (1966) calculated for NGC 7762. In addition to this, the distance and metal abundance estimation of NGC 7762 by Patat & Carraro (1995) are in agreement with the distance and metal abundance of V731 Cep found in this study. The most reliable evidence that V731 Cep is evaporated from NGC 7762 can be obtained from the spatial distribution and the metallicity of V731 Cep.

In calculation of the kinematical properties of V731 Cep, the systemic velocity, distance and proper motion components listed in Table 8 were used in the algorithm given by Johnson & Soderbloom (1987). The computed space velocity components with their errors are given in Table 8. The total space velocity of 14 km s^{-1} for V731 Cep is in agreement with the space velocities of young stars. Although the space velocity of the cluster could not be computed due to its unavailable RV data, the

[3] http://stev.oapd.inaf.it/∼lgirardi/cgi-bin/param

distance of 55 pc between V731 Cep and NGC 7762, and similar age and metallicity distribution of V731 Cep with NGC 7762, suggest that V731 Cep could be evaporated from NGC 7762. However, it is necessary to carry out precise photometric and spectroscopic observations of the member stars of NGC 7762 in order to form more definite conclusions on the history of V731 Cep in relation with NGC 7762.

Acknowledgements
The authors would like to thank to Dr. Antonio Cabrera-Lavers for his help in extracting extinction data from RC stars and to the referee, Prof. E. F. Guinan, for his useful comments that improved the readability of this paper. This study is part of a project funded by ÇOMU Scientific Research Foundation under project code BAP2008/37. The research of MW was supported by the Research Program MSM0021620860 of the Ministry of Education of Czech Republic. Participation of MZ in this study was endorsed by the grant GA CR 205/06/0217 of the Czech Science Foundation.

REFERENCES

Ak T., Bilir S., Ak S., Retter A., 2007, NewA, 12, 446
Alves D. R., 2000, ApJ, 539, 732
Andersen J., 1991, A&ARv, 3, 91
Bahcall J.N., Soneira R.M., 1980, ApJS, 44, 73
Bakış V., Erdem A., Budding E., Demircan O., 2003, IBVS, 5381
Bakış V., Bakış H., Tüysüz M., Özkardeş B., Erdem A., Çiçek C., Demircan O., 2005a, IBVS, 5616
Bakış V., Doğru S.S., Bakış H., Doğru D., Erdem A., Çiçek C., Demircan O., 2005b, IBVS,5662
Bakış V., Bakış H., Budding E., Demircan O., Zejda M., 2007, in Solar and Stellar Physics Through Eclipses (ASP Conf. Ser.: San Francisco), eds. O. Demircan, S.O. Selam and B. Albayrak, 370, 213
Bakış V., Bakış H., Demircan O., Eker Z., 2008, MNRAS, 384, 1657
Bilir S., Güver T., Aslan M., 2006, AN, 327, 693
Bilir S., Ak T., Soydugan E., Soydugan F., Yaz E., Filiz Ak N., Eker Z., Demircan O., Helvacı M., 2008, AN (in press) (astro/ph: 2008arXiv0806.1290)
Cabrera-Lavers A., Garzón F., Hammersley P. L., 2005, A&A, 433, 173
Chincarini G., 1966, MmSAI, 37, 423
Claret A., 2004, A&A, 424, 919
Cutri R. M., et al., 2003, The IRSA 2MASS All-Sky Point Source Catalog, NASA/IPAC Infrared Science Archive. http://irsa.ipac.caltech.edu/applications/Gator/
da Silva L., Girardi L., Pasquini L., Setiawan J., von der Lühe O., de Medeiros J. R., Hatzes A., Döllinger M. P., Weiss A., 2006, A&A, 458, 609
Drimmel R., Cabrera-Lavers A., López-Corredoira M., 2003, A&A, 409, 205
Fiorucci M., Munari U., 2003, A&A, 401, 781
Fitzgerald M. P., 1970, A&A, 4, 234
Giménez A., Garcia-Pelayo J.M., 1983, Ap&SS, 92, 203
Giménez A., 1985, ApJ, 297, 405
González J. F., Lapasset E., 2003, A&A, 404, 365
Grocholski A. J., Sarajedini A., 2002, AJ, 123, 1603
Johnson H. L., Morgan W. W., 1953, ApJ, 117, 313
Johnson D. R. H., Soderblom D. R., 1987, AJ, 93, 864
Jørgensen B. R., Lindegren L., 2005, A&A, 436, 127
Kurucz R. L., 1993, CD-ROM 13, 18, http://kurucz.harward.edu
Kwee K. K., van Woerden, H., 1956, BAN, 12, 327
Lacy Claud H. S., 1992, AJ, 104, 2213
Latham D. W., Nordstroem B., Andersen J., Torres G., Stefanik R. P., Thaller M., Bester M. J., 1996, A&A, 314, 864
Lee J. W., Kim C.-H., Koch R. H., 2007, MNRAS, 379, 1665
López-Corredoira M., Cabrera-Lavers A., Garzón F., Hammersley P. L., 2002, A&A, 394, 883
Metcalfe T. S., Mathieu R. D., Latham D. W., Torres G., 1996, ApJ, 456, 356
Patat F., Carraro G., 1995, A&AS, 114, 281
Pejcha O., 2005, IBVS, 5645
Pietrzyński G., Gieren W., Udalski A., 2003, AJ, 125, 2494
Salaris M., Girardi L., 2002, MNRAS, 337, 332
Southworth J., Smalley B., Maxted P. F. L., Claret A., Etzel P. B., 2005, MNRAS, 363, 529
Southworth J., Clausen J. V., 2007, A&A, 461, 1077
Straižys V., Kuriliene G., 1981, Ap&SS, 80, 353
van Hamme W., 1993, AJ, 106, 2096
Wainscoat R. J., Cohen M., Volk K., Walzer H. J., Schwartz D. E., 1992, ApJS, 83, 111
Wilson R. E., Devinney E. J., 1971, ApJ, 166, 605
Wilson R. E., 1994, PASP, 106, 921
Yi S., Demarque P., Kim Y., Lee Y., Ree C. H., Lejeune T., Barnes S., 2001, ApJS, 136, 417
Zacharias N., Monet D.G., Levine S.E., Urban S.E., Gaume R., Wycoff G.L., 2005, Naval Observatory Merged Astrometric Dataset (NOMAD), Vizier, http://cdsarc.u-strasbg.fr/viz-bin/Cat?I/297
Zahn J.P., 1977, A&A, 57, 383
Zejda M., 2004, IBVS, 5583
Zucker S., Mazeh T., 1994, ApJ, 420, 806